Tahir and Piracha, J Material Sci Eng 2019, 8:1
DOI: 10.4172/2169-0022.1000511

Journal of Material Sciences & Engineering

Research Article Open Access

Influence of Undoped and Cu^{+2}/Fe^{+3} Codoped ZnO Nanoparticles on Enhanced Photocatalytic Evaluation Using Textile Dye

Muhammad Mubeen Tahir* and Javed Latif Piracha

Department of Mechanical Engineering, Mirpur University of Science and Technology (MUST), Mirpur, Azad Kashmir, Pakistan

Abstract

Pure and Cu^{+2}/Fe^{+3} codoped ZnO nanoparticles were synthesized by polyol method. X-rays diffraction, scanning electron microscopy, dispersion X-rays spectroscopy; UV-Vis spectroscopy and photoluminescence were used for the characterization of the as synthesized nanoparticles. X-ray diffraction study of as synthesized nanoparticles presented the hexagonal wurtzite phase of ZnO structure. Optical studies revealed a blue shift in the absorption spectrum when ZnO was doped with Cu^{+2}/Fe^{+3}.

The degradation rate of disperse blue dye using ZnO and codoped ZnO nanoparticles were considered under the solar region. ZnO and codoped ZnO degrade dye under consideration however, codoped ZnO nanoparticles proved to be extra efficient catalyst as compared to ZnO nanoparticles. The kinetic study of the dye was also calculated and it was observed that degradation of the respective dye followed pseudo first-order kinetics. The as-synthesized nanoparticles prove to be environment-friendly and active and can be vastly used for the purification of water polluted by different dyes that are carcinogenic in nature.

Keywords: ZnO; Cu^{+2}/Fe^{+3}-ZnO; Photocatalysis; Disperse blue

Introduction

As the revolution in science and technology is increasing day by day, the demand for novel materials that can be used in various industrial methods increases. Among different materials organic dyes are most important that could be used in different methods like leather, textile, tanneries, cosmetic, pharmaceuticals, nourishment handling and rural research. Based on their huge scale generation and broad functions, organic dyes are the main constituent of industrial wastewater [1,2]. Wastewater from the processing of dye mostly comprises residue of dyestuffs, colour intermediates and in addition crude materials such as aromatic amines and inorganic sodium salts. Human beings as well as aquatic life are greatly affected by such toxins present in ground and surface water. Some of them are cancer-causing as well as mutagenic and hence, some special treatment for water purification is quite important [3].

Different methods have been applied for the removal of coloured impurities from the wastewater for the satisfaction of many severe ecological systems. Physical and biological methods have been used till now however, there are many drawbacks of these methods. Likewise, these techniques are not able to entirely remove the dye molecules and significant amount of sludge is formed which cause secondary pollution [4,5]. In recent years an alternative to conventional methods, is "Advanced Oxidation Processes" (AOPs) in which highly reactive species like such as hydroxyl radicals (-OH), superoxide anion radicals (O^{2-}) and hydrogen peroxide (H_2O_2) are produced that are considered as initiators of the oxidative degradation [6,7].

The heterogeneous photocatalysis, belonging to the AOPs, is a useful and environmentally caring technology, which can be conveniently applied for the degradation of dye pollutants [8,9]. This process gains much importance since sunlight can be used for it. The chief drawback of AOPs is their high cost (costly reactants such as H_2O_2 and UV generation). Hence, the use of catalysis and solar energy could be helpful in the improvement of the applications [10].

Various wide band gap semiconductor photocatalysts, such as TiO_2 [11], ZnO [12], SnO_2 [13], ZnS [14], CdS [15], ZnS and Fe_2O_3 [16] have been used for this process. Among them, ZnO is a widely investigated photocatalyst as it is non-hazardous to the environment, cheap, and has excellent oxidizing nature with high stability [17,18]. The use of ZnO is hindered by some apparent drawbacks: (i) High recombination of photogenerated electron-hole, (ii) Constricted light receptive range, and (iii) Photo corrosion. To overcome the mentioned limitations, various strategies such as incorporation of ZnO i.e. doping, and combination of semiconductor oxides with metals and non-metals have been carried out [19].

The better surface area of the nanostructured ZnO have the ability of photocatalytic degradation of dyes [20]. The fluorescent and various surface defects of the ZnO nanostructures can be improved by incorporation of metal ions into the ZnO lattice. Additionally, various properties of ZnO are expected to be changed by doping of metal ions including the absorptivity. Recently, simultaneous doping of two kinds of atoms (co-doping) have gained much importance due to the fact that it can result in improved photocatalytic activity and specific properties as compared to the incorporation of the metal oxides with a single element [21]. This mixed oxide possesses the combination of properties that neither individual possesses. The suitable band gap of mixed oxide allows absorption in visible region which covers the most of the part of solar light.

Numerous techniques have been used for the preparation of ZnO nanoparticles like co-precipitation [22], polyol [23], solvothermal [24], hydrothermal [25], non-aqueous chemical method [26], and chemical

***Corresponding author:** Muhammad Mubeen Tahir, Department of Mechanical Engineering, Mirpur University of Science and Technology (MUST), 10250, Mirpur, Azad Kashmir, Pakistan; E-mail: mubeentahir66@gmail.com

Received December 17, 2018; **Accepted** February 12, 2019; **Published** February 19, 2019

Citation: Tahir MM, Piracha JL (2019) Influence of Undoped and Cu^{+2}/Fe^{+3} Codoped ZnO Nanoparticles on Enhanced Photocatalytic Evaluation Using Textile Dye. J Material Sci Eng 8: 511. doi: 10.4172/2169-0022.1000511

bath deposition [27]. Among these different methods, the polyol method is quite feasible due to uniform shape, narrow size distribution, and a low degree of agglomeration of as-synthesized nanoparticles [28]. Mostly poly-alcohol like Ethylene Glycol (EG), Diethylene Glycol (DEG) or 1, 2-propanediol are applied in this method both as solvent and capping agent [29].

The aims of our study are: (a) To synthesize ZnO nanoparticles from Zinc acetate dihydrate) by polyol method, (b) To co-dop the as synthesized ZnO nanoparticles with Cu^{+2} and Fe^{+3} using Copper nitrate trihydrate and ferric chloride, (c) To characterize the morphology and structure of the prepared nanoparticles with several physical methods (SEM, XRD, EDX and UV) and (d) To investigate the photocatalytic degradation kinetics using disperse blue dye whose structural formula is represented in Figure 1.

Experimental Procedure

Chemicals

Copper nitrate trihydrate ($Cu(NO_3)_2.3H_2O$), Zinc acetate dihydrate ($Zn(CH_3COO)_2.2H_2O$) and Iron (III) chloride obtained from Merck, Ethylene glycol (EG) 99%, Poly (vinylpyrrolidone) PVP obtained from Daejung Reagent Chemicals-Korea. Acetone, distilled water, ethanol are the analytical reagents. Disperse blue dye, used for photocatalytic degradation and was used as received.

Apparatus

UV-Visible absorption spectra were measured by using SHIMADZU UV 1800 Spectrophotometer. The morphology of the as-synthesized nanoparticles was characterized by FESEM TESCAN MIRA3XMU Scanning Electron Microscope (SEM) together with EDX (JEOL, USA). The crystallinity of as synthesized nanoparticles were studied by Philips MPD-X' Pert (XRD2) with Cu-Kα radiation (λ=0.154178 nm). The photocatalytic activities of pure and Cu^{+2}/ Fe^{+3} codoped Zinc oxide nanoparticles were determined contrary to the removal of model dye i.e. disperse blue solution with 0.16 g photocatalyst as well as in the absence of photocatalyst after regular time intervals.

Sample preparation

Polyol method was applied for the preparation of ZnO nanoparticles. 15 mL of Ethylene Glycol was added in a round bottom flask and heated to reach 170°C. The temperature is stabilized at 170°C and then 0.1 M PVP was added in EG glycol followed by the addition of 0.1 M Zinc Acetate solution. The resulting solution is heated for 3 hours while keeping the temperature constant.

After 3 hours the white suspension of the mixture was added with acetone and washed by ethanol and water. Similarly, 2 mL of 0.01 M Copper and Iron Acetate were used for doping of Fe^{+3}/Cu^{+2} under same conditions as used for ZnO nanoparticles formation.

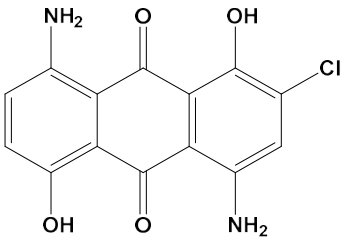

Figure 1: Chemical structure of Disperse Blue dye.

Photocatalytic activity evaluation

In order to estimate the photocatalytic action of pure and codoped ZnO nanoparticles at room temperature, aqueous solution of disperse blue was selected.

In this process, the catalytic reaction was carried out in a beaker that contains 40 ppm of dye solution and 0.15 g of catalyst. The dye solution and suspension were homogenized by stirring for 15 min and then exposed to visible light radiation. The photocatalytic reactions were carried out in opened space where it was possible to collect the solar radiation properly. The test samples from the beakers were taken at regular intervals and centrifuged at 4000 rpm for 10 min to remove the nanocatalysts. The degradation was observed by measuring the absorbance at wavelength of 560 nm. The catalytic effectiveness was expressed in terms of percentage photodegradation of the dye (disperse blue), which has been calculated using the formula:

$$\text{Percentage degradation}(\%) = \frac{Co - Ct}{Co} \times 100 \quad (1)$$

Where Co is the initial concentration of dye solution and Ct is the concentration after a time 't'.

Results and Discussions

The crystal structure of as-synthesized ZnO nanoparticles is clearly revealed by X-ray diffraction (Figure 2). The peaks at 2θ values 31.72, 34.40, 36.21, 47.41 and 56.51 corresponds to (100), (002), (101), (102) and (110) crystal planes. The XRD patterns for both the samples were same with hexagonal wurtzite phase (01-080-0075) with no extra peak which may be ascribed to the incorporation of Cu and Fe ions into the Zn lattice. X'Pert High Score version 2.0a software was used for the determination of Full Width at Half Maximum (FWHM) of the diffraction line and crystallite size was calculated by using the Scherrer formula. The average particle size calculated was found to be 28 nm and 13.98 nm for ZnO and Cu^{+2}/ Fe^{+3}co-doped respectively.

$$D = k\lambda / (\beta \cos\theta) \quad (2)$$

where D is crystallite size, λ is the wavelength of X-rays, k is a constant, β is full width at half-maximum of the diffraction peak and θ is angle of diffraction.

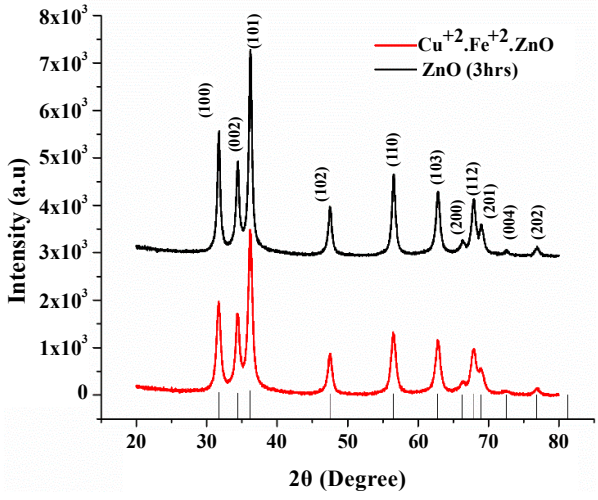

Figure 2: X-rays diffraction pattern of undoped and Cu^{+2}/Fe^{+3} ZnO nanoparticles.

The size and overall morphology of the nanoparticles were studied by scanning electron microscopy. ZnO (Figures 3a and b) nanoparticles show very clear morphology having circular structure of the crystals with variable size from 1 μm to 200 nm. A high degree of particle agglomeration is observed, which is in agreement with literature [30]. Figures 3c and d shows the SEM images of codoped ZnO with mixed morphology of nanoparticles. The particles have mostly spherical geometry and the size of the particles ranges from few micrometres to 300 nm. The SEM images of pure and codoped ZnO nanoparticles can be clearly distinguished as codoped ZnO do not have any large sized spherical nanoparticles as depicted by ZnO images.

Chemical compositional study of the undoped and Cu^{+2}/Fe^{+3} codoped ZnO nanocatalysts has been carried out by EDX. It is mostly used to analyse the amount of Cu^{+2} and Fe^{+3} elements present in $Zn_{1-x}Cu_xFe_xO$ sample. The typical EDX spectra of undoped and co-doped nanoparticles and their elemental compositions are given in Figure 4. The EDX analysis proves the existence of Cu and Fe in the ZnO lattice and atomic % age is almost equal to the stoichiometric calculation within the experimental error. So, the experimental concentration of the dopant is in good agreement with their EDX spectra.

Optical study

The UV–Visible absorption spectrum of the undoped and Cu^{+2}/Fe^{+3} codoped ZnO nanoparticles have been performed using UV Visible spectrophotometer from 300 to 800 nm and are shown in Figure 5. ZnO nanoparticles showed an absorption peak at 370 nm and Cu^{+2}/Fe^{+3} co-doped ZnO at 359 nm respectively. The peak at 359 nm exhibits a clear shift owing to doping of Cu^{+2}/Fe^{+3} in the ZnO structure. There is no extra peak for metallic copper which shows that both the elements are doped in the ZnO and are not present in the form of any impurity. The optical band gap was calculated by using the Tauc relation and represented in Figure 6.

$$\alpha h\gamma = A^* (h\gamma - Eg)^n$$

where α is the optical absorption coefficient, h γ is the energy of incident photon, Eg is the band gap energy of samples under observation.

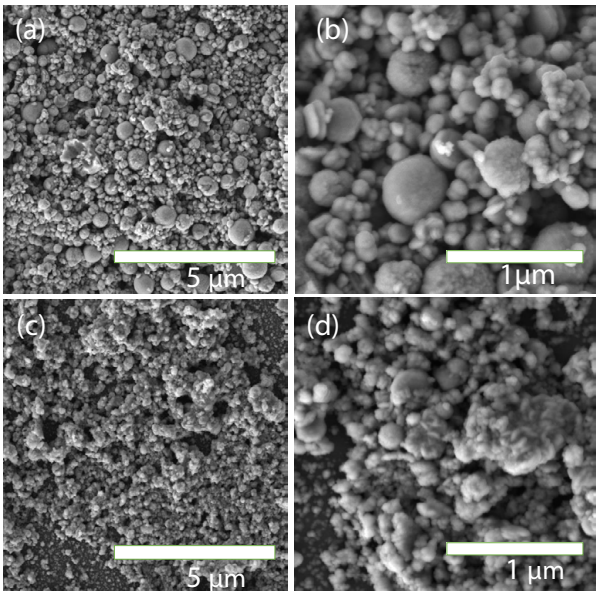

Figure 3: SEM images of pure and codoped ZnO at two different magnifications.

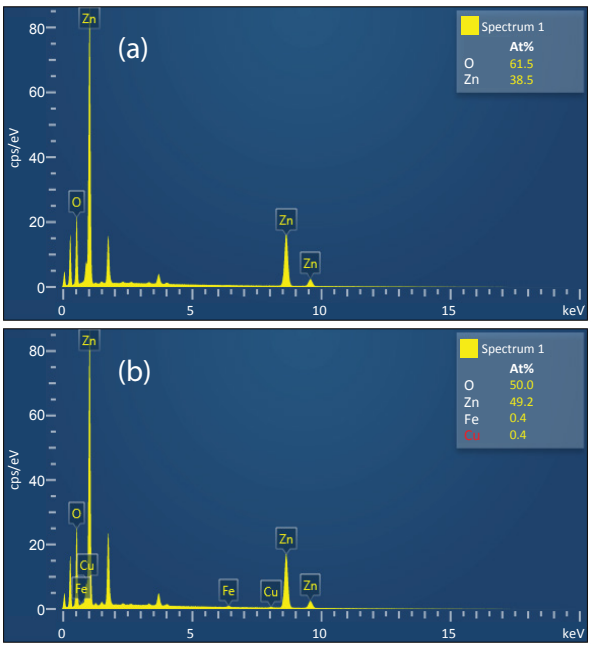

Figure 4: EDX spectra of ZnO and Cu^{+2}/Fe^{+3} codoped ZnO with their atomic percentages.

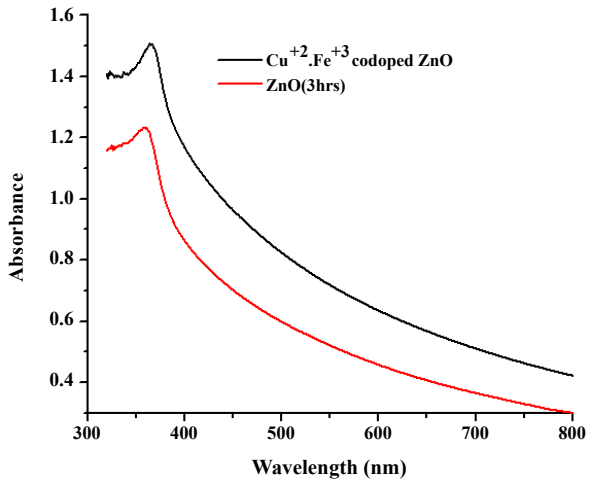

Figure 5: UV-Vis. Spectra of Pure and $Cu^{+2}.Fe^{+3}$ codoped ZnO nanoparticles.

The band gap of the undoped and codoped ZnO nanocatalysts can be obtained by plotting (αhγ) versus hγ. The band gap of ZnO nanoparticles was found to be 3.08 eV and for Cu^{+2}/Fe^{+3}codoped ZnO nanoparticles 2.96 eV respectively. The experimental red shift in the band gap is because of the doping of Cu^{+2} and Fe^{+3} with even distribution in structure of ZnO. The decrease of band gap is also because of the strong p–d mixing of O with Fe and Cu [31].

Photodegradation experiments

The experiments for solar photocatalytic degradation of the dye disperse blue were performed under bright sunshine. The degradation rate was observed by the change in absorbance at 560 nm for disperse blue dye. The calibration curve for this dye is given in the Figure 7.

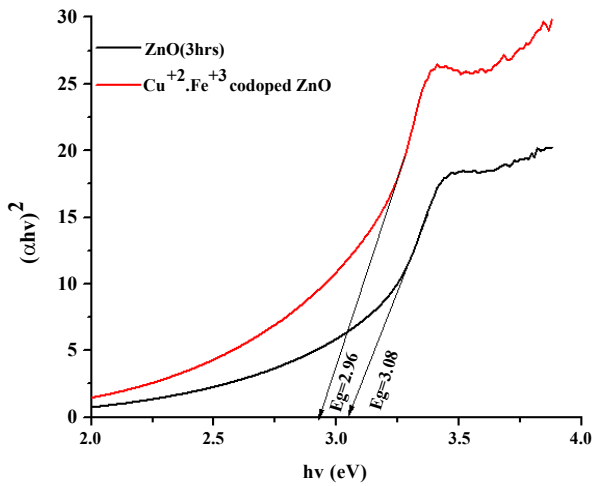

Figure 6: Tauc Plot showing band gaps of ZnO and Cu^{+2}/Fe^{+3}-ZnO nanoparticles.

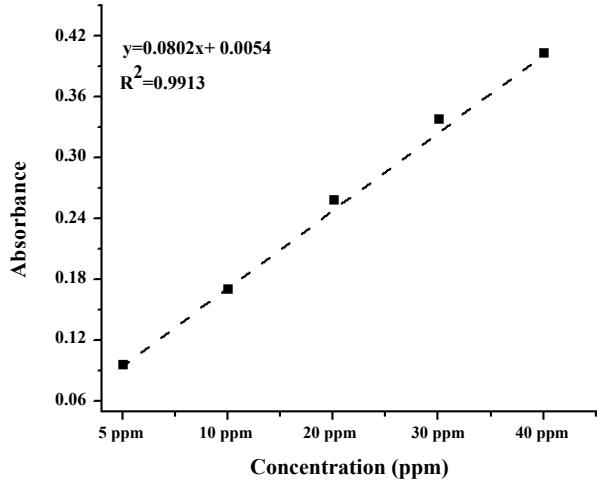

Figure 7: Calibration curve for the dye, disperse blue used for photocatalytic degradation.

Initial experiment was performed with the dye solution without any catalyst under direct illumination of solar light. The irradiations were applied for one hour to notice whether there is any degradation effect. This was carried out due to the fact that various dyes were degraded when exposed to direct UV light in a short period of time even in the absence of catalyst. But, there were negligible change observed for the duration of about 1 hour (<10%). This revealed that the organic compounds in the dye solution were very stable and do not have ability of self-destruction even it was radiated under UV light for an hour. However, after addition of photocatalysts into the solution, the absorption peak at 580 nm dropped significantly. The adsorption of the dye over the photocatalysts was monitored under the following conditions (sunlight/ZnO, sunlight/ZnO/Cu^{+2}/Fe^{+3}, sunlight/dye solution and Dark/ZnO) at definite concentrations of dye solution and photocatalyst loaded. In order to check the degradation effect, the dye was irradiated to sunlight for 50 min. It was noticed that as the concentration of the dye solution decreases, the decrease in the absorption peak was observed and is depicted in (Figures 8a-d). The decrease in the adsorption peak at 580 nm shows that the organic compound in the dye solution is decomposed.

The percentage degradation of the dye under various situations are showed in the Figure 9. As the amount of photocatalyst was increased, the efficiency of degradation is increased to a certain limit and then it decreases slowly. With increase in the photocatalyst concentration above 0.10 g/L, decrease in percentage degradation was observed because of dispersion of light and poor penetration rate through the solution. The degradation rate of the dye using ZnO, Cu^{+2}/Fe^{+3}-. ZnO nanocatalysts under different experimental conditions were 78.25%, 98.32% and 61.51% respectively.

The order of reaction was also calculated by applying pseudo-first-order kinetic model on ZnO and Cu^{+2}/Fe^{+3}-ZnO nanocatalysts and is commonly stated by the following relation.

$$\ln\left(\frac{Ct}{Co}\right) = kt$$

Where k is the rate of photodegradation constant (min^{-1}) and Ct and Co are the concentrations (mg/L) of dye at time 't' and primarily used. A straight line was obtained by plotting ln (Ct/C0) versus time of reaction t which proves that the reaction follows a pseudo-first-order kinetics behaviour [31,32] and is presented in Figure 10.

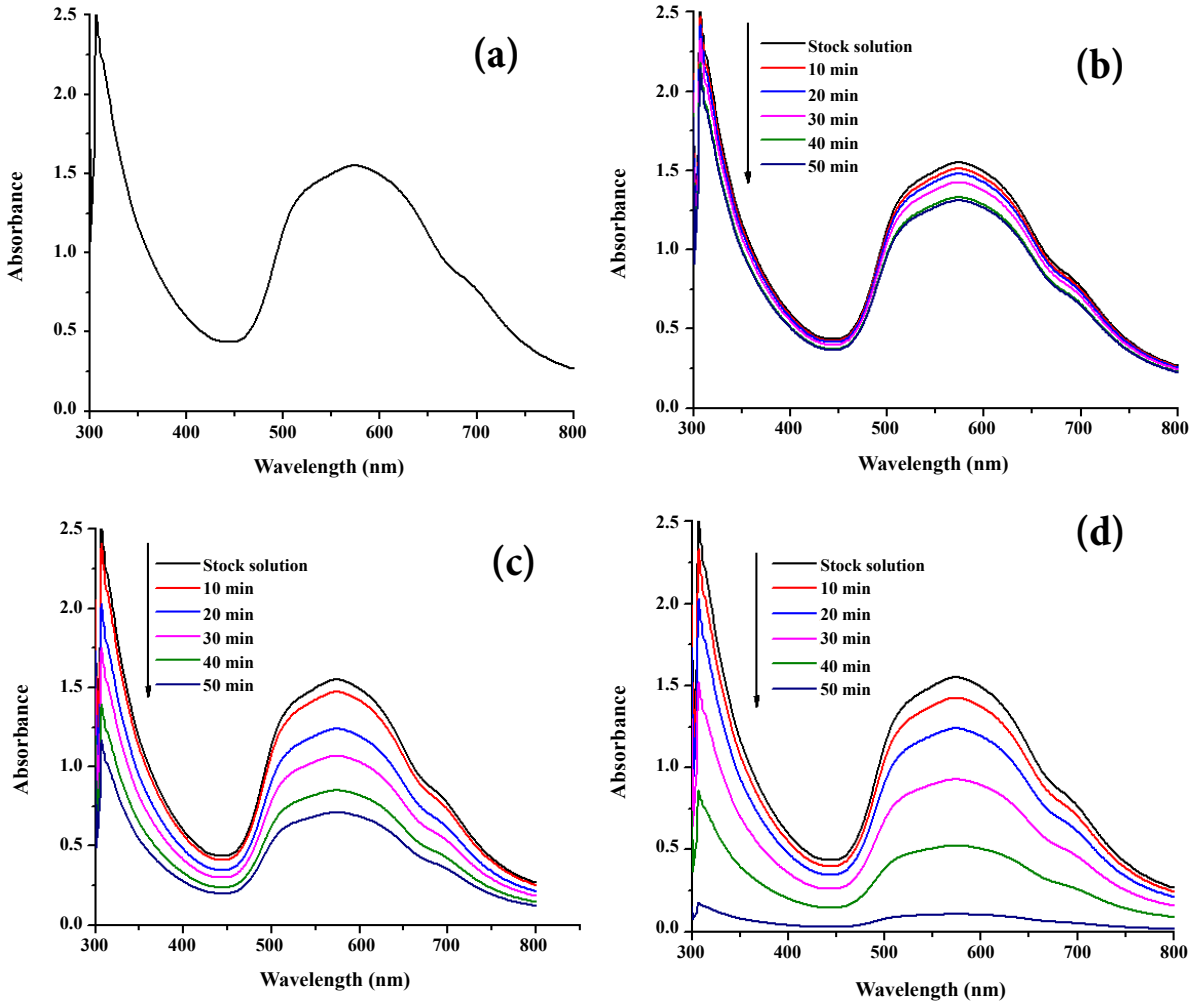

Figure 8: UV–Vis absorbance spectra of (a) Disperse blue solution, (b) Dye solution in the presence ZnO in Dark, (c) Dye solution in the presence of ZnO, (d) Dye solution in the presence of Cu^{+2}/Fe^{+3}-ZnO nanoparticles.

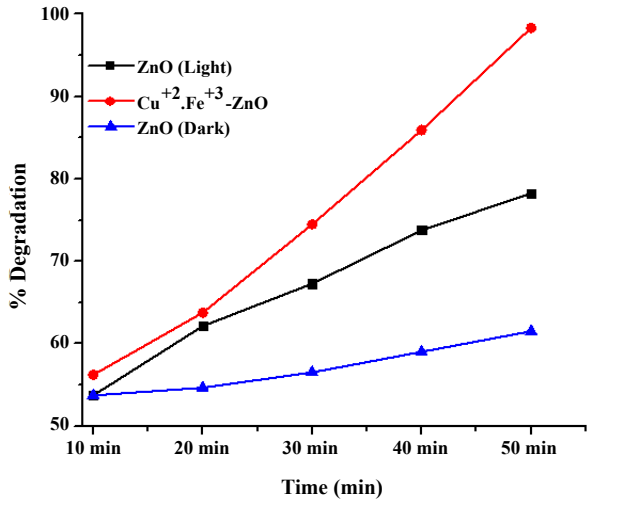

Figure 9: Percentage degradation of disperse blue at various conditions (50 ppm dye solution, 0.15 g catalyst amount, room temperature).

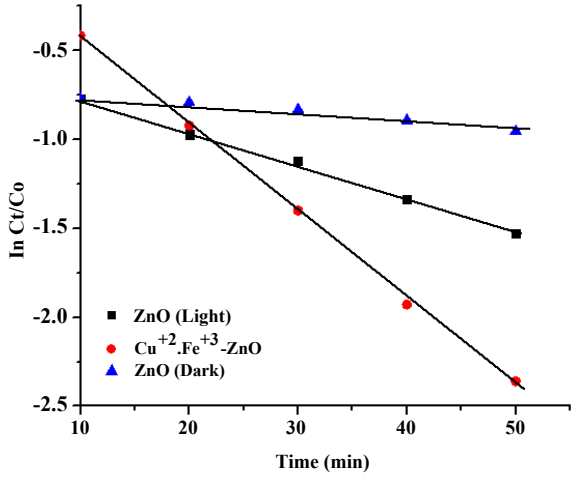

Figure 10: Kinetic curves for photocatalytic degradation of disperse blue at different conditions (50 ppm initial concentration of solution, 0.15 g amount catalyst, room temperature).

The correlation coefficients (R^2) were higher than 0.9913, which shows that the photodegradation of the dye under consideration fits well with the kinetic model. The rate constants of the dye in the presence of ZnO/light, Cu^{+2}/Fe^{+3}-ZnO /light are 0.1877 and 0.4855 min^{-1}, respectively.

Conclusion

Pure and codoped ZnO nanoparticles were synthesized by using polyol method. The wurtzite structure for as synthesized nanoparticles was confirmed by XRD patterns. The morphology and the size of ZnO crystal was confirmed by SEM analysis. The UV-Visible results revealed that there was a red shift in absorption in case of dopant as compared to pure ZnO with a decrease in band gap from 3.308 (for ZnO) to 2.96 eV (for Cu^{+2}/Fe^{+3} doped) ZnO nanocatalysts. Photocatalytic measurements showed that increase in Cu^{+2}/Fe^{+3} doping in the ZnO nanoparticles results enhanced photocatalytic activity.

References

1. Lam SM, Sin JC, Abdullah AZ, Mohamed AR (2012) Degradation of wastewaters containing organic dyes photocatalysed by zinc oxide: A review. Desalin Water Treat 41: 131-169.
2. Chakrabarti S, Dutta BK (2004) Photocatalytic degradation of model textile dyes in wastewater using ZnO as semiconductor catalyst. J Hazard Mater 112: 269-278.
3. Kumaran NN, Muraleedharan K (2017) Photocatalytic activity of ZnO and Sr2+ doped ZnO nanoparticles. Journal of Water Process Engineering 17: 264-270.
4. Bouberka Z, Benabbou KA, Khenifi A, Maschke U (2014) Degradation by irradiation of an Acid Orange 7 on colloidal TiO2/(LDHs). J Photochem Photobiol A: Chem 275: 21-29.
5. Pamecha K, Mehta V, Kabra BV (2016) Photocatalytic degradation of commercial textile Azo Dye Reactive Blue 160 by heterogeneous photocatalysis. Advanced Applied Science and Research 7: 95-101.
6. Chong MN, Jin B, Chow CW, Saint C (2010) Recent developments in photocatalytic water treatment technology: A review. Water Res 44: 2997-3027.
7. Sotto A, Lopez-Munoz MJ, Arsuaga JM, Aguado J, Revilla A (2010) Membrane treatment applied to aqueous solutions containing atrazine photocatalytic oxidation products. Desalin Water Treat 21: 175-180.
8. Borges ME, Sierra M, Cuevas E, García RD, Esparza P (2016) Photocatalysis with solar energy: sunlight-responsive photocatalyst based on TiO2 loaded on a natural material for wastewater treatment. Sol Energy 135: 527-535.
9. Rajamanickam D, Shanthi M (2016) Photocatalytic degradation of an organic pollutant by zinc oxide–solar process. Arab J Chem 9: S1858-S1868.
10. Malato S, Maldonado MI, Fernandez-Ibanez P, Oller I, Polo I, et al. (2016) Decontamination and disinfection of water by solar photocatalysis: The pilot plants of the Plataforma Solar de Almeria. Mat Sci Semicon Proc 42: 15-23.
11. He F, Li J, Li T, Li G (2014) Solvothermal synthesis of mesoporous TiO2: The effect of morphology, size and calcination progress on photocatalytic activity in the degradation of gaseous benzene. Chem Eng J 237: 312-321.
12. Yu C, Cao F, Li G, Wei R, Jimmy CY, et al. (2013) Novel noble metal (Rh, Pd, Pt)/BiOX (Cl, Br, I) composite photocatalysts with enhanced photocatalytic performance in dye degradation. Sep Purif Technol 120: 110-122.
13. Wang X, Fan H, Ren P (2013) Electrospinning derived hollow SnO2 microtubes with highly photocatalytic property. Catal Commun 31: 37-41.
14. Chen F, Cao Y, Jia D (2013) A facile route for the synthesis of ZnS rods with excellent photocatalytic activity. Chem Eng J 234: 223-231.
15. Radeka M, Markov S, Lončar E, Rudić O, Vučetić S, et al. (2014) Photocatalytic effects of TiO2 mesoporous coating immobilized on clay roofing tiles. J Eur Ceram Soc 34: 127-136.
16. Behnajady MA, Modirshahla N, Shokri M, Zeininezhad A, Zamani HA (2009) Enhancement photocatalytic activity of ZnO nanoparticles by silver doping with optimization of photodeposition method parameters. J Environ Sci Health A 44: 666-672.
17. Wang Y, Ren P, Feng C, Zheng X, Wang Z, et al. (2014) Photocatalytic behavior and photo-corrosion of visible-light-active silver carbonate/titanium dioxide. Mater Lett 115: 85-88.
18. Wei BX, Zhao L, Wang TJ, Gao H, Wu HX, et al. (2013) Photo-stability of TiO2 particles coated with several transition metal oxides and its measurement by rhodamine-B degradation. Advanced Powder Technology 24: 708-713.
19. Cho S, Jang JW, Kim J, Lee JS, Choi W, et al. (2011) Three-dimensional type II ZnO/ZnSe heterostructures and their visible light photocatalytic activities. Langmuir 27: 10243-10250.
20. Yang JL, An SJ, Park WI, Yi GC, Choi W (2004) Photocatalysis using ZnO thin films and nanoneedles grown by metal–organic chemical vapor deposition. Adv Mater 16: 1661-1664.
21. Subash B, Krishnakumar B, Velmurugan R, Swaminathan M, Shanthi M (2012) Synthesis of Ce co-doped Ag–ZnO photocatalyst with excellent performance for NBB dye degradation under natural sunlight illumination. Catal Sci Technol 2: 2319-2326.
22. Chauhan R, Kumar A, Chaudhary RP (2013) Visible-light photocatalytic degradation of methylene blue with Fe doped CdS nanoparticles. Appl Surf Sci 270: 655-660.
23. Aydiner C, Kaya Y, Beril Gönder Z, Vergili I (2010) Evaluation of membrane fouling and flux decline related with mass transport in nanofiltration of tartrazine solution. J Chem Technol Biotechnol 85: 1229-1240.
24. Jing Z, Tan L, Li F, Wang J, Fu Y, et al. (2013) Photocatalytic and antibacterial activities of CdS nanoparticles prepared by solvothermal method. NISCAIR Online Periodicals Repository pp: 57-62.
25. Liu SH, Qian XF, Yin J, Ma XD, Yuan JY, et al. (2003) Preparation and characterization of polymer-capped CdS nanocrystals. J Phys Chem Solids 64: 455-458.
26. Pattabi M, Amma BS, Manzoor K (2007) Photoluminescence study of PVP capped CdS nanoparticles embedded in PVA matrix. Mater Res Bull 42: 828-835.
27. Pawar RC, Lee JY, Kim EJ, Kim H, Lee CS (2012) Synthesis of CdS with graphene by CBD (chemical bath deposition) method and its photocatalytic activity. Korean Journal of Materials Research 22: 504-507.
28. Fiévet F, Brayner R (2013) The polyol process. In Nanomaterials: A Danger or a Promise? Springer, London, pp: 1-25.
29. Couto GG, Klein JJ, Schreiner WH, Mosca DH, de Oliveira AJ, et al. (2007) Nickel nanoparticles obtained by a modified polyol process: synthesis, characterization, and magnetic properties. J Colloid Interface Sci 311: 461-468.
30. Borges ME, Sierra M, Cuevas E, García RD, Esparza P (2016) Photocatalysis with solar energy: Sunlight-responsive photocatalyst based on TiO2 loaded on a natural material for wastewater treatment. Sol Energy 135: 527-535.
31. Ferhat M, Zaoui A, Ahuja R (2009) Magnetism and band gap narrowing in Cu-doped ZnO. Appl Phys Lett 94: 142502.
32. Chen X, Wu Z, Liu D, Gao Z (2017) Preparation of ZnO photocatalyst for the efficient and rapid photocatalytic degradation of azo dyes. Nanoscale research letters 12: 143.